Journal of Applied Mechanics and Technical Physics, Vol. 40, No. 3, 1999

SELF-EXCITED OSCILLATIONS IN RAREFIED IMPACT SUPERSONIC JETS

G. F. Gorshkov and V. N. Uskov

UDC 533.6.011.72

The effect of rarefaction on self-excited oscillations in impact supersonic jets (underexpanded jets interacting with a normally located, planar, bounded obstacle) is investigated. Amplitude-frequency characteristics of pressure fluctuations at the obstacle are obtained.

It is known that in impact supersonic jets with certain combinations of the working parameters, sharp transitions from steady to unsteady flow occur [1–4], and strong self-excited oscillations arise.

It should be noted that most of the results obtained, except for those of [5], refer to dense jets at stagnation pressures $p_0 \gg 10^5$ Pa. In many practical problems, however, a jet discharges from a nozzle into a rarefied medium at much smaller values of p_0. Under these conditions, the gas jet flow is highly affected by viscosity and rarefaction [6, 7], which can be defined by the complex $\mathrm{Re}_L = \mathrm{Re}_* N^{-0.5}$, where $N = p_0/p_\infty$ is the expansion ratio, p_∞ is the ambient pressure, and Re_* are the Reynolds numbers calculated from the gas parameters in the critical section of the nozzle.

As shown in [8], a decrease in the density of a free immersed jet with finite off-design parameter n and a Mach number $\mathrm{M}_a = 2$ (in contrast to $\mathrm{M}_a = 1$) leads to a decrease in the diameter of the Mach disk, displacement of it from the nozzle, and formation of shock waves of a periodic structure (X-shaped configuration). In this transition, the distance to the point of reflection increases by 10–15% [7] compared to calculations, and the radial dimensions of the jet do not depend on Re_L.

At fixed distance from the nozzle exit to the obstacle h and off-design parameter n (flow around an unbounded obstacle [8]), as rarefaction increases, the central shock (CS) originating ahead of the obstacle recedes from the nozzle and, in some cases, a shock-wave pattern (SWP) of X-shaped configuration occurs. The effect of rarefaction on the SWP is most pronounced for numbers $\mathrm{Re}_L < 100$. The obstacle shifts the boundary of transition to the X-shaped structure toward smaller Re_L.

Thus, transition to flow with an unperturbed first side lobe occurs nonmonotonically: initially, the displacement of the CS from the nozzle shifts this transition toward larger values of h, and then a decrease in the diameter of the barrel shock shifts it toward smaller h [8].

The effects of viscosity and rarefaction are most pronounced in the subsonic region of the shock-layer flow — between the CS and the obstacle [9, 10]. However, for jets with $\mathrm{M}_a = 2$ and $\mathrm{Re}_L > 150$, the flow type in an impact jet, as in the case of dense jets, is determined only by the geometrical similarity parameter $H = h/x_*$ [10], where $x_* = 2r_a \mathrm{M}_a(\gamma n)^{0.5}$. The indicated features of interaction must also be manifested in unsteady flow around the obstacle. In this connection, we formulate the problem to be studied as follows: study the effect of rarefaction on the qualitative and quantitative characteristics of self-excited oscillations by changing Re_L.

The experiments described here were performed with a GURS-1 vacuum facility, which incorporates an evacuated chamber with a volume of 10 m^3, two VN-6 forevacuum pumps, and a BN-15000 booster pump. The low-pressure chamber is provided with a remotely controlled three-degree traverse gear, to which an obstacle in the form of a cylinder with a 16-mm-diameter planar edge was attached. An IS-2156 piezoelectric

Baltiisk State Engineering University, St.-Petersburg 198005. Translated from Prikladnaya Mekhanika i Tekhnicheskaya Fizika, Vol. 40, No. 3, pp. 109–115, May–June, 1999. Original article submitted April 4, 1997; revision submitted July 8, 1997.

0021-8944/99/4003-0455 $22.00

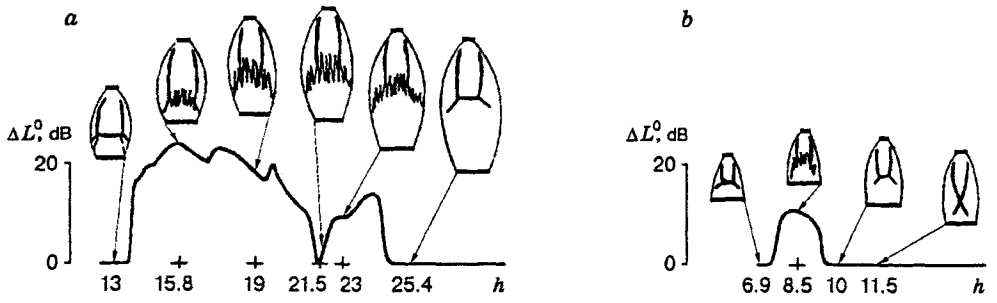

Fig. 1

pressure transducer was located at the center of the obstacle. The static pressure at the obstacle was recorded by a DMI transducer through an orifice located at 2 mm from the center.

The jets were produced by a conical Laval nozzle with a geometric Mach number $M_a = 2$, critical cross-sectional diameter $d_* = 4$ mm, and a cone semivertex angle of 15°. The nozzle was screwed in a receiver to which the working gas (air) entered from the facility space. In the experiments, we measured the total p_0 and static p pressures in the receiver and at the obstacle, the external pressure in the low-pressure chamber p_∞, and the pressure fluctuations $p(\tau)$ at the obstacle.

The critical Reynolds numbers Re_* were varied by changing p_0 at constant p_∞, which was ensured by allowing air to bleed into the low-pressure chamber through backing pumps at constant volume flow rate of the gas.

The pressure p_∞ was measured by a DMI differential transducer relative to a basic pressure $p_b = 10$ Pa, which was produced by evacuating one of the transducer cavities by an NVZ-20 vacuum pump and maintained constant when the pump operated in the non-flow regime. The pressure in this cavity was measured by a PMT-2 thermocouple transducer with a VT-3 vacuum gauge, graded by a McLeod gauge. Pressures above 200 Pa were also measured by U-shaped dibuthylphthalate manometers. The error in determining pressures of $10\text{–}3 \cdot 10^4$ Pa was 5%.

The instantaneous magnitude of the fluctuations of $p(\tau)$ from the IS-2156 transducer amplified by a 00011 microphone amplifier of a 01021 noise meter made by RFT (passband 200 kHz) was recorded on the tape of an NO-67 magnetograph (frequencies 40 kHz). During the experiment, we determined the integral level of pressure fluctuations (at the exit from the indication unit 02022) $\Delta L^0 = 20 \log(\sigma/p_w) - L_n$, where σ is the effective value of $p(\tau)$, $p_w = 2 \cdot 10^{-5}$ Pa is the acoustic pressure at the hearing threshold, and L_n is the broadband noise level. The frequency range of the dynamic channel "gauge–noise meter–magnetograph is not lower than 40 kHz with nonuniformity of the amplitude–frequency characteristic (AFC) for the indicated frequency range ±3 dB.

The qualitative pattern of underexpanded rarefied jet flow around the obstacle is obtained by visualization using a glow discharge with subsequent photorecording of it on a film. For analysis of the AFC of the self-excited oscillations, we used the same apparatus set and procedure of data processing as in [1, 5]. The experiments were performed for the following parameters: $\gamma = 1.4$, $T_0 = 293$ K, $p_0 = (0.86\text{–}6.5) \cdot 10^3$ Pa, $n = p_a/p_\infty = 2\text{–}13.5$, $Re_* = (0.59\text{–}3.84) \cdot 10^3$, $Re_L = 114\text{–}371$, $h = 2\text{–}30$, and radius of the obstacle $R = 3.08$ (here and below, all linear dimensions are referred to the radius of the nozzle exit r_a).

According to the estimate of rarefaction in [9], the range of Knudsen numbers $Kn = (0.67\text{–}5.1) \cdot 10^{-3}$ is such that the flow around the obstacle is continual, and the effects of viscosity and rarefaction are concentrated in the wall boundary layer. The CS can be considered isolated (unsmeared), i.e., it is a gas-dynamic discontinuity on which the Rankine–Hugoniot relations are satisfied.

Figure 1 illustrates the change of the SWP in the impact rarefied jet obtained by flow visualization using a glow discharge as the obstacle continuously recedes from the nozzle exit h (the curve in Fig. 1a corresponds to $Re_L = 371$ and $n = 13.5$ and the curve in Fig. 1b corresponds to $Re_L = 162$ and $n = 2.6$). Curves of the integral level at the center of the obstacle ΔL^0 versus h are also given here. Analysis of Fig. 1 shows

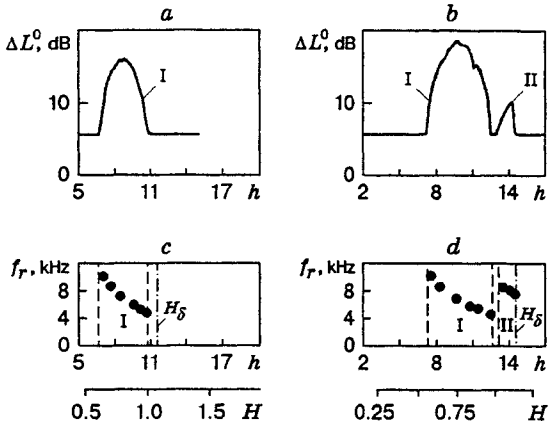

Fig. 2

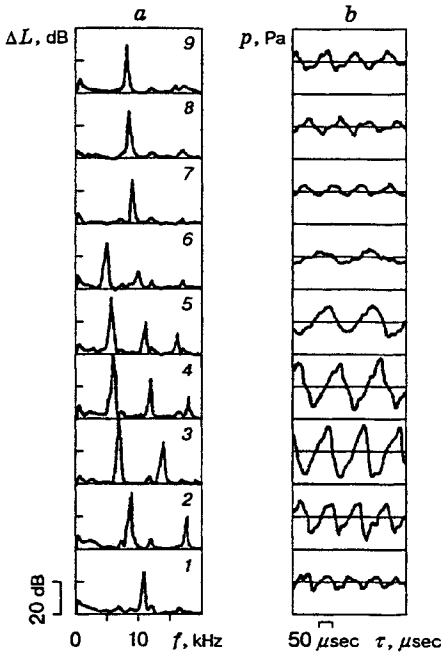

Fig. 3

that a smooth increase in h leads to a sudden decay of the steady flow: in the impact system "jet–obstacle," self-excited oscillations arise which are accompanied by a considerable increase in the integral level ΔL^0 (the curve in Fig. 1a corresponds to the maximum value $\Delta L^0 = 24$ dB and the curve in Fig. 1b corresponds to $\Delta L^0 = 10$ dB). However, in contrast to the flow of dense jets around an obstacle [1–4], the second unsteady regime is detected at certain combinations of the parameters Re_L and n.

Analysis of the integral level ΔL^0 (the curves in Fig. 2a and b) and the frequency (the points in Fig. 2c and d) of pressure fluctuations (the fundamental tone) at the center of the obstacle as functions of the distance $h(H)$ revealed two types of flow around a bounded obstacle: type A, for which the first (I) and second (II) regimes of self-excited oscillations occur (Fig. 2b and d; $\mathrm{Re}_L = 184$ and $n = 7.5$), and type B, for which only the first regime is present (Fig. 2a and c; $\mathrm{Re}_L = 165$ and $n = 5.1$). The occurrence of either of these regime depends on the combination of the parameters M_a, H, and Re_L (see Fig. 1).

Thus, for type A, the first regime is characterized by the presence of several discrete components (discrete tone: along with the fundamental tone there are overtones) in the frequency spectrum (Fig. 3a, curves 1–6), strong oscillations in the SWP (see Fig. 1a), and pressure at the obstacle (Fig. 3b) of large amplitude and rather low frequency f. The pressure oscillations have a pronounced periodic structure (curves 1–9 in Fig. 3b correspond to distances h and the parameters of Fig. 2b and d). The regime is characterized by considerable extension H.

The second regime, for which the level ΔL^0 and extension H are much smaller (by three times) than those for the first), is characterized by a single discrete component of the frequency spectrum (Fig. 3a, curves 7–9), moderate oscillations in the SWP, and pressure at the obstacle. The regime is sensitive to the variation in the parameter Re_L.

The segments of variation in the integral level $\Delta L^0 = \Delta L^0(H)$ (see Fig. 2a and b) have sharp boundaries (the dashed curves in Fig. 2c and d correspond to the beginning and end of self-excited oscillations $H_{\mathrm{ib,e}}$). The experiment showed that transition from the first regime to the second can occur at a small interval H (about $0.1H$) (Fig. 2b) or immediately one after the other (see Fig. 1a).

Within the indicated range of parameters, the second regime occurs at rather large n, such that the CS diameter is comparable (equal) to the diameter of the obstacle: ($n = 13.5$–5.8 and $\mathrm{Re}_L = 371$–169), (5.24

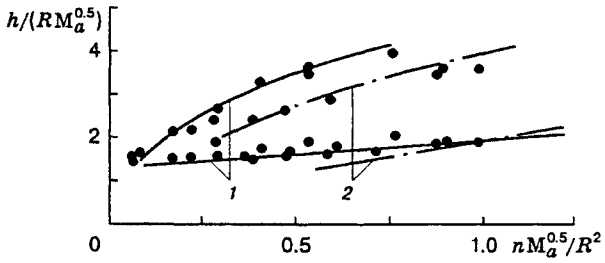

Fig. 4

and 231), and (4.5 and 214). The end of the second regime always corresponds to occurrence of flow with an unperturbed first side lobe ($H_{2e} = H_\delta$ the dot-and-dashed curve in Fig. 2d). This is indicated by both the measured average pressure at the center of the obstacle and visualization of the SWP (see Fig. 1a).

For type B (see Fig. 2a and c), the first regime is also characterized by the presence of a discrete tone in the frequency spectrum and strong oscillations in the SWP and obstacle pressure of large amplitude and rather low frequency. The oscillations have a pronounced periodic structure. The regime is rather extended in H, as in the case of dense impact jets.

When the obstacle moves from the nozzle, the regime always terminates before transition to radial flow with unperturbed first side lobe: $H_{1e} < H_\delta$ (Fig. 1b and the dashed and dot-and-dashed curves in Fig. 2c). When the obstacle moves to the nozzle exit, the beginning of the unsteady regime (its end for motion from the nozzle) coincides with the moment of "collapse" of the flow with unperturbed first side lobe because of the experimentally detected hysteresis of the average pressure at the obstacle (H_δ is shifted toward the nozzle).

A single self-oscillating regime occurs for such values of n for which the CS diameter is much smaller than the diameter of the obstacle or they are comparable but the rarefaction parameter Re_L is small and influences the second regime ("eats" it up): ($n = 6.6$ and $\mathrm{Re}_L = 147$), (4.8 and 126), (4.3 and 172), (3.5 and 189), (3.3 and 189), and (2.6 and 163).

Occurrence of self-excited oscillations for both types of unsteady flow can be accompanied by a rather smooth and sharp increase in the integral level ΔL^0. Transition from the second regime to flow with unperturbed first side lobe proceeds jumpwise (see Fig. 2b). As H increases within the limits of existence of each of the regimes, the fundamental frequency of pressure oscillations at the obstacle f_r (the first discrete component of the frequency spectrum) decreases monotonically, and in transition from the first to the second regime there is a jumpwise increase in f_r (Fig. 2c and d). The sawtooth variation in f_r corresponds to the variation in f_r for dense jets flowing around an unbounded obstacle [1].

Figure 4 shows the boundaries of the regions of existence of self-excited oscillations in the generalized coordinates used in [4] for dense jets. The boundary values of $H_{ib,e}$ were determined from the increase and damping of the curves of $\Delta L^0 = \Delta L^0(H)$ (see Fig. 2a and b), which corresponded to the appearance of a strong discrete component in the spectra of pressure fluctuations on the obstacle.

Analysis of the data showed that despite some quantitative differences in the extension of the unsteady flow zones, the results obtained (the points in Fig. 4 correspond to the distances h at which self-excited oscillations occur; the lower curve 1 is the averaged boundary of the beginning of self-excited oscillations and the upper curve is the boundary of the end) are in agreement with the results for self-excited oscillations for dense supersonic impact jets [1–4] (curves 2), and the zones of the first and second regimes are located within the characteristic boundaries.

An important feature of the jet interaction is the hysteresis phenomena originating in the shock layer when the obstacle performs quasisteady motion relative to the nozzle exit (its motion from the nozzle or toward it). For fixed initial parameters M_a, γ, n, and Re_L, it is established experimentally that for rarefied impact jets, hysteresis for the level of ΔL^0 (in contrast to the averaged pressure on the obstacle) does not exist for all types of flow around the obstacle.

The influence of rarefaction on self-excited oscillations is manifested as follows. For large values of

Re_L, the boundaries of existence of self-excited oscillations do not depend on Re_L but are determined by the parameters obtained for dense impact jets [1, 2]. A decrease in values $\mathrm{Re}_L < 371$ (increase of rarefaction) can lead not only to quantitative variation in the extension of the regions of existence of self-excited oscillations but also to disappearance of initially the second and then the first regimes. This is associated with both transition to the X-shaped structure of shock waves in a rarefied jet (see Fig. 1b), and smearing of the SWP of the first side lobe of the jet [7]. A decrease in the density in a free immersed jet with $\mathrm{M}_a = 2$ for $n = \mathrm{const}$, as noted above, leads to a decrease in the diameter of the Mach disk, displacement of the Mach disk from the nozzle, and formation of the resulting periodic structure of shock waves [8].

At $\mathrm{Re}_L \leqslant 172$ ($n = 6.6$–2.6) there is a single (first) regime, and at $\mathrm{Re}_L < 121$ self-excited oscillations are not detected, which agrees with [5]. The disappearance of the second region is caused by a decrease in the cross dimension of the shock layer (decrease in the Mach disk in the jet) in transition to the periodic structure of shock waves for fixed diameter of the obstacle.

Hence, for jets with a finite off-design parameter, unsteady regimes can occur when the values of Re_L are larger than a certain minimum Re_L^0. According to [5], for an unbounded obstacle at $\mathrm{M}_a = 2$, $\mathrm{Re}_L^0 = 128$ for the first regime and $\mathrm{Re}_L^0 = 150$ for the second. A certain increase in the limiting and other boundary values of Re_L compared with those indicated above is due to both the difference between the impact systems considered and to the smaller range of n. It is reasonable to assume that for smaller values of n, transition to the X-shaped configuration can occur at larger Re_L.

Frequency analysis of the unsteady processes showed that for the first regime of self-excited oscillations, the frequency spectrum (see curves 1–6 in Fig. 3a) contains several discrete components that exceed (by up to 40 dB) the general level of continuous noise of the jet. For the second there is a single component which exceeds the general broadband background by 25–30 dB. In each of the regimes, the frequency spectra are shifted toward lower frequencies with increase in H (curves 1–6). For the second regime, "recovery" of the frequency f_r to the initial values proceeds jumpwise (curve 7).

On the segments of onset and termination of the self-excited oscillation regime, the spectra show just one discrete component (curves 1 and 6), which also far exceeds the broadband background) (22–25 dB). The occurrence of overtones in the frequency spectrum is a consequence of the nonsinusoidal pressure fluctuations caused by shock-wave processes in the region between the CS and the obstacle.

The parameters of the system "CS–obstacle" exert an effect on the frequency of pressure oscillations. An increase in the recession of the CS from the obstacle Δ with increase in the distance h within the limits of the self-excited oscillation region is accompanied by a decrease in the frequency of the fundamental tone f_r. An increase in n and M_a [1–4] acts in the same direction. Taking into account the aforesaid and introducing the complex $d_a n^{0.5}$ as the transverse dimension of the shock layer, we can generalize the frequency characteristics of self-excited oscillations for Strouhal numbers Sh_r for both regimes by the universal empirical formula

$$\mathrm{Sh}_r^{-1} = a_0/(f_r d_a n^{0.5}) = A_i \Delta/(d_a n^{0.5}) + B_i,$$

where $A_1 = 4.3$ and $B_1 = 1.2$ (the first regime), $A_2 = 1.3$ and $B_2 = 1.4$ (the second regime), a_0 is the velocity of sound of the stagnation flow, and Δ is the distance from the obstacle about which the CS oscillates before the obstacle (the middle position Δ is taken from [2]).

The experiments were performed with the participation of A. V. Savin and V. S. Favorskii.

REFERENCES

1. G. F. Gorshkov, V. N. Uskov, and V. S. Favorskii, "Nonstationary flow of underexpanded jet around an unbounded obstacle," *Prikl. Mekh. Tekh. Fiz.*, **34**, No. 4, 58–65 (1993).
2. V. A. Ostapenko and A. V. Solotchin, "Force action of an underexpanded supersonic jet on a plane obstacle," *Izv. Sib. Otd. Akad. Nauk SSSR, Ser. Tekh. Nauk*, No. 13, Issue 3, 26–32 (1974).
3. V. N. Glaznev, "Self-excited oscillations in discharge of off-design supersonic jets," *Model. Mekh.*, **1**, No. 6, 29–43 (1987).

4. G. V. Naberezhnova and Yu. N. Nesterov, "Unstable interaction of a rarefied supersonic jet with an obstacle," *Tr. TsAGI*, No. 1765, 3–23 (1976).
5. A. V. Savin, E. I. Sokolov, V. S. Favorskii, and I. V. Shatalov, "Influence of rarefaction on the unsteady interaction of an underexpanded supersonic jet with a perpendicular obstacle," *Prikl. Mekh. Tekh. Fiz.*, No. 6, 78–83 (1991).
6. V. S. Avduevskii, É. A. Ashratov, A. V. Ivanov, and U. G. Pirumov, *Supersonic Nonisobaric Gas Jets* [in Russian], Mashinostroenie, Moscow (1985).
7. N. I. Kislyakov, A. K. Rebrov, and R. G. Sharafutdinov, "On the structure of high-head jets of low density behind a hypersonic nozzle," *Prikl. Mekh. Tekh. Fiz.*, No. 2, 42–52 (1975).
8. E. I. Sokolov and I. V. Shatalov, "Flow ahead of an obstacle for a perpendicular low-density jet discharging from a supersonic nozzle," in: *Jet Flows of Liquids and Gases* [in Russian], Part 1, Novopolotsk Polytechnical Institute, Novopolotsk (1982), pp. 129–132.
9. I. V. Shatalov, "Flow in the region of interaction of an underexpanded rarefied jet with a planar obstacle perpendicular to the jet axis," *Prikl. Mekh. Tekh. Fiz.*, No. 2, 115–120 (1985).
10. E. I. Sokolov and I. V. Shatalov, "Flow similarity parameters for the interaction of an underexpanded supersonic jet with a perpendicular planar obstacle," in: *Dynamics of Inhomogeneous and Compressible Media* (collected papers) [in Russian], Izd. Leningrad Univ., Leningrad, No. 8, 175–183 (1984).